Involvement of TLR4 Signaling Regulated-COX2/PGE2 Axis in Liver Fibrosis Induced by *Schistosoma japonicum* Infection

Lan Chen
Guangzhou Medical University
Xiaofang Ji
Guangzhou Medical University
Manni Wang
Guangzhou Medical University
Xiaoyan Liao
Guangzhou Medical University
Cuiying Liang
Guangzhou Medical University
Juanjuan Tang
Guangzhou Medical University
Zhencheng Wen
Guangzhou Medical University
Ferrandon Dominique
Universite de Strasbourg
Zi Li (lizi1002@gzhmu.edu.cn)
Sino-French Hoffmann Institute

Research

Keywords: TLR4 signaling, COX2/PGE2 axis, liver fibrosis, Schistosoma japonicum

Posted Date: January 6th, 2021

DOI: https://doi.org/10.21203/rs.3.rs-139573/v1

Version of Record: A version of this preprint was published at Parasites & Vectors on May 25th, 2021. See the published version at https://doi.org/10.1186/s13071-021-04790-7.

Abstract

Background: The hepatic stellate cells (HSCs) activation plays pivotal role in hepatic inflammation and liver fibrosis.TLR4 pathway activation has been reported to be involved in mice liver fibrosis induced by hepatitis virus infection, alcohol abuse, biliary ligation, carbon tetrachloride 4 treatment and *Schistosoma japonicum* (*Sj*) infection. The effect and mechanisms of cyclooxygenase 2 (COX2)/prostanoid E2 (PGE2) axis on liver fibrosis induced by *Sj* are still unclear.

Results: This study investigated the link between COX2/PGE2 axis and TLR4 signaling in the induction of liver fibrogenesis in mice during *Sj* infection and in vitro culturing hepatic stellate cells (HSCs) strain-LX-2. The COX2/PGE2 axis was positively related with *Sj*-induced liver fibrosis. TLR4 pathway activation stimulated the COX2/PGE2 axis, in *Sj*-infected mice andin lipopolysaccharide (LPS)-exposed cultured HSCs. Synthetic PGE2 activated culturing HSCs through up-regulating alpha smooth muscle actin (α-SMA) expression. In LPS-triggered HSCs, NS398, a COX2 inhibitor led to suppression of PGE2 synthesis and reduced expression of α-SMA and type I collagen (COL I).

Conclusions: These results indicated firstly the positive association of COX2/PGE2 axis with liver fibrosis induced by *Sj* infection. TLR4 signaling may control COX2/PGE2 axis in *Sj*-infected mice liver and in vitro culturing HSCs at least partially. COX2/PGE2-EP2/EP4 axis might be good drug targets against liver fibrosis induced by *Sj* infection.

Introduction

Prostaglandin E2 (PGE2) is produced when arachidonic acid is released from the plasma membrane and metabolized by two types of cyclooxygenases (COXs), COX-1 and COX2. Three distinct PGE2 synthases (PGES) contribute specifically to PGE2 synthesis. Membrane-bound PGES-2 (mPGES-2) and cytosolic PGES-1 (cPGES-1) are constitutively expressed and functionally coupled to COX-1 for maintenance of basal levels of PGE2, while mPGES-1 is frequently induced concomitantly with COX2 by various pro-inflammatory stimuli thereby generating a transient spike in PGE2 levels [1]. PGE2 is actively transported out of cells by multiple drug resistance-associated protein 4 (MRP4) and enters into the extracellular microenvironment, where PGE2 binds with four cognate EP receptors (EP1-EP4) and initiates diverse biological signaling pathways. Alternatively, PGE2 is transported into cells via the prostaglandin transporter (PGT)[2].Via the PGE2 receptors EP2 and EP4 that trigger downstream cAMP signaling, PGE2 stimulates inflammation, pain, proliferation of certain cell types such as smooth muscular cells, plasticity, and cell injury [3, 4].

Activated but not quiescent HSCs of mice express COX2 [5, 6]. Interestingly, the association of COX2 and its dependent PGE2-EP2&EP4 axis with fibrogenesis remains controversial. A selective COX2 inhibitor, NS-398, blocked the induction of α-SMA, PGE2 in a human HSC cell line, LI90 [5, 7]. The COX2 inhibitor, SC-236, also lowered the extent of CCl4-induced rat liver fibrosis [8].Celecoxib, another specific inhibitor of COX2, alleviated the rat liver fibrosis induced by thioacetamide (TAA) through decreased intrahepatic and

intestinal LPS levels [9]. The COX2/PGE2 axis is positively associated with choline-deficient, L-amino acid-deficient diets (CDAA)-, TAA- and bile duct ligation (BDL)-induced rat liver fibrosis [10, 11] and liver cirrhosis in rats, mice, and patients [9, 12]. In contrast, all organs from CCl4-treated mice had elevated PGE2 levels [12], yet the COX2/PGE2 axis protected against fibrosis in the lungs [13]and kidneys [14]. Furthermore, several studies indicated that the COX2/PGE2 axis counteracted hepatic fibrogenesis by inhibiting the proliferation, contractility, and migration of HSCs and decreasing the production of ECM [15, 16]. *Schistosoma japonicum* (*Sj*) infection is still existed in 12 provinces in China. Infection of *Sj* leads to severe liver fibrosis induced by eggs trapped in the liver. The role and mechanisms of COX2/PGE2 axis in *Sj*-induced liver fibrosis are still unclear.

Hepatic fibrosis is the common pathophysiologic process resulting from chronic liver injury and inflammation. Hepatic stellate cells (HSCs) transdifferentiate into alpha smooth muscle actin (α-SMA)-expressing myofibroblasts, which proliferate and secrete inflammatory cytokines and produce excessive extracellular matrix (ECM) including collagen type I (COL I) and type III (COL III). These three molecules constitute hallmarks of liver fibrosis [17]. TGF-β1 signaling activation is a well-known mechanism that mediates HSCs activation [18]. TGF-β1 of the parasite origin correlated with the extent of *Sj*-induced liver fibrosis [19]. Recent studies suggested that pathogen-associated molecular patterns (PAMPs), gut microflora-derived bacterial products such as lipopolysaccharide (LPS), bacterial DNA, and endogenous substances released from damaged cells, known as damage or danger-associated molecular patterns (DAMPs), activate hepatic TLRs that contribute to the development of liver fibrosis [20]. Activated HSCs express high levels of TLR4 [21].Reported mechanisms of TLR4 signaling-induced HSCs activation & liver fibrosis include: 1) Bambi down regulation, a TGF-β signaling inhibitor in quiescent HSCs [22, 23]; 2) miR-29 down regulation, which targets COL I expression [24]; 3) increased levels of LPS & DAMPs directly activating TLR4 signaling thereby activating nuclear factor κB (NF-κB) and c-Jun N-terminal kinase (JNK) that induce the production of many pro-inflammatory chemokines like monocyte chemoattractant protein-1 (MCP-1) and CCL-5, which in turn promote HSCs activation [25, 26]. We have showed that the positive feedback regulation between transglutaminase 2 (TGM2) and TLR4 signaling in HSCs correlated with liver fibrosis post Sj infection [27].

TLR4 signaling controls the activation of COX2-PGE2 pathway in macrophages [16, 28], intestinal epithelial cells [29], esophagus [30], and auditory cells [31]. Both TLR4 signaling and COX2/PGE2 axis are involved in HSCs activation and hepatic fibrosis. However, no research has reported whether there is a link between the COX2/PGE2 axis and TLR4 signaling pathway in HSCs activation and fibrogenesis during *Sj* infection. Our work aimed to investigate the role of COX2/PGE2 axis in *Sj*-induced liver fibrosis and whether the relationship between it and TLR4 signaling is the mechanism.

Materials And Methods

Reagents

NS398, the inhibitor of COX2 activity was ordered from MedChemExpress (HY-13913, New Jersey, USA). TAK242, a TLR4 inhibitor was purchased from Shanghai Haoyuan Chemoexpress (Shanghai, China). Trizol was obtained from Life Technologies (Waltham, USA). SYBR® Premix Ex Taq™ II (RR820A) and PrimeScript™ RT reagent Kit with gDNA Eraser (RR047A) were from TaKaRa Biotechnology Co. Ltd. (Dalian, China). The antibodies used were as follows: anti-COX2 (12282, Cell Signaling Technology, USA), anti-mPGES-1 (160140, Cayman, USA), anti-EP1(ab217925, Abcam, USA), anti-EP2 (ab167171, Abcam, USA), anti-EP3 (SC-20676, Santa Cruz Biotechnology, USA), anti-EP4 (SC-55596, Santa Cruz Biotechnology, USA), anti-GAPDH (ab181603, Abcam, USA), anti-α-SMA (BS70000,Bioworld,USA), anti-Col I (BA0325, BOSTER, USA), anti-TLR4 (ab47093, Abcam, USA), anti-p65 (6956, Cell Signaling Technology, USA), anti-p-p65 (3033, Cell Signaling Technology, USA), and anti-β-Tubulin (DKM9003, Sanjian Biotechnology, China). HRP-conjugated secondary antibodies of mice or rabbit IgG (35552 and 35510, Invitrogen, Waltham, USA). Bicinchoninic acid (BCA) Protein Assay Kit was purchased from GuangzhouDingguo Biotechnology (Guangzhou, China). Polyvinylidene fluoride membrane (PVDF) (ISEQ00010) was purchased from Merck Millipore (Darmstadt, Germany). 3,3'-diaminobenzidine (DAB) substrate kit was purchased from Gene Tech Company Limited (Shanghai, China). Enhanced ECL reagent was from GBCBIO Technologies, Guangzhou, China. Sirius red staining (connective tissue staining) kit was purchased from Abcam (ab150681, USA). Lipopolysaccharide (LPS) and synthetic prostaglandin E2 (PGE2) were ordered from Sigma-Aldrich, USA. DMEM medium was from ThermoFisher (Gibco), fetal bovine serum (FBS) was from ExCell Bio. ELISA kit for LPS levels detection was from Elabscience (E-EL-0025c, Wuhan, China). Ribo FECT CP Transfection Kit was from Robibio Biotechnology Limited (C10511, Guangzhou, China).

Mice, parasite infection and NS398 treatment

Six-to eight-week-old female C57BL/6 mice were obtained from the SPF Biotechnology Co. Ltd (Beijing) and maintained according to institutional guidelines. All mice were approved to be appropriate and humane by the Institutional Animal Care and Use Committee at South China Agricultural University. Mice were infected per-cutaneously through the abdomen with 20 ± 3 *Sj* cercariae of the Chinese mainland strain. The mice developed advanced fibrosis at week 8 post-infection (n = 5). The uninfected mice were used as normal controls (n = 9). We treated mice with NS398 (3 mg/kg body weight, n = 5) in 2%DMSO by intraperitoneal injection 3 times a week from week 5 to week 7, while the infection control group (n = 5) only received 2%DMSO. Two non-infected control mice groups were treated with NS398 (n = 5) and 2%DMSO (n = 6) respectively. Elsewhere, 4-week post-infection, mice were injected through the intraperitoneal route twice a week for 4 weeks with 100 μl TAK242 (0.3 mg/kg body weight) dissolved in PBS (n = 8), while the infection control group (n = 7) only received PBS. Two non-infected control mice groups were treated with TAK242 (n = 7) and PBS (n = 7) respectively. Mice were sacrificed at week 8 after *Sj* infection and liver tissues were collected for further analysis.

RNA isolation and quantitative reverse transcription PCR

Total RNA was extracted from fresh mice livers using Trizol reagent. Genomic DNA was removed, and then cDNA was synthesized using PrimeScript™ RT reagent Kit with gDNA Eraser. The relative RNA

expression level of target genes was measured by real-time quantitative reverse transcription polymerase chain reaction (RT-qPCR) with SYBR® Premix Ex Taq™ II kit and the CFX96™ real-time system according to the manufacturer's procedure. The RT-qPCR primer pairs were listed in Table 1. The RNA expression level of each gene was normalized to GAPDH and analyzed using the 2 − ΔΔCt data analysis method.

Table 1
Primer pairs' sequences of mice genes used in RT-qPCR

Proteins	Genes	Forward primer sequence	Reverse primer sequence
GAPDH	*Gapdh*	TGTGTCCGTCGTGGATCTGA	TTGCTGTTGAAGTCGCAGGAG
COX2	*COX2*	TTCCAATCCATGTCAAAACCGT	AGTCCGGGTACAGTCACACTT
mPGES-1	*Ptges*	CACACTGCTGGTCATCAAGAT	TCACTCCTGTAATACTGGAGGC
EP1	*Ptger1*	TGCTTGCCATCGACCTAGC	CACCCAGGAAATGACACGC
EP2	*Ptger2*	CAGCTCGGTGATGTTCTCGG	GAGCACCAATTCCGTTACCAG
EP3	*Ptger3*	CAGCTCATGGGGATCATGTGT	CTCAACCGACATCTGATTGAAGA
EP4	*Ptger4*	CTTGTTGGTAAGCCCGGTGA	AGACCCGACAGACCGAAGAA
MRP4	*Abcc4*	GGCACTCCGGTTAAGTAACTC	TGTCACTTGGTCGAATTTGTTCA
PGT	*Slco2a1*	CGACTCCTCCTGTATCCGGT	TGTTCTTCTTCACCCTCCAGC

Abbrev: GAPDH &*Gapdh*, glyceraldehyde-3phosphate dehydrogenase; COX, cyclooxygenase; mPGES-1, microsomal prostaglandin E synthase-1; Ptges, prostaglandin E synthase; EP1 & Ptger1, prostaglandin E receptor 1; MRP4, multidrug resistance-associated protein 4; *Abcc4*, ATP binding cassette subfamily C member 4; PGT, prostaglandin transporter; *Slco2a1*, Solute carrier organic anion transporter family member 2A1.

Sirius red staining

Fresh hepatic tissues were fixed in 4% paraformaldehyde for 24 h, and then embedded with paraffin. The 4 μm liver sections were prepared and stained with Sirius red to semi-quantify the extent of collagen deposition, which demonstrates the severity of liver fibrosis. The collagen deposition area of *Sj* single egg granuloma as displayed in deep red was measured and analyzed by Image J software. Each section was evaluated in double-blind fashion by two independent researchers.

Western blotting

The proteins from culturing LX-2 cells or mice liver tissue were extracted and equal quantities of total proteins lysate were resolved on 10% SDS-polyacrylamide gels and then transferred to PVDF membranes. After incubation with the indicated primary and secondary antibodies, the target proteins were visualized using an enhanced ECL reagent.

Immunohistochemical (IHC) assay

Endogenous peroxidase in mouse liver sections was blocked with 3% hydrogen peroxide (H_2O_2). Immunohistochemical (IHC) staining assay was used to determine the expression level and location of α-SMA and Col I in the mice liver tissue using anti-α-SMA (1:200) and anti-Col I (1:400) primary antibodies, followed by HRP-conjugated secondary anti-rabbit or anti-mouse antibodies. The images were observed and captured with an optical microscope equipped with a camera (Olympus, Tokyo, Japan). The semi-quantitative analysis was determined by image J software [27].

Cell culture and treatment

A human HSCs line, LX-2 was cultured in DMEM medium with 10% fetal bovine serum (FBS).When the confluence reached 80–90%, LX-2 cells were exposed to LPS or syntheticPGE2, or these cells were pretreated by TAK242 for 30 minutes or NS398 for 15 minutes at the indicated concentrations prior to stimulation with LPS.

RNA interference

LX-2 cellswere seeded in a six-well plate the day before transfection at 30–50% confluency. TLR4-specific small interfering RNAs (siRNA), or negative control siRNAs, synthesized by Robibio Biotechnology Limited, were transfected using the Ribo FECT CP Transfection Kit according to the manufacturer's instructions. 24 hours after transfection, cells were treated with LPS or mock-treated for 24 hours. Total protein of cells in RIPA lysis buffer with PMSF were then extracted to be measured by western blotting. TLR4 siRNA sequences are as follows: TLR4 siRNA-1, 5'- GGACAACCAGCCTAAAGTA – 3'; TLR4 siRNA-2, 5'- GGTGTGAAATCCAGACAAT – 3'.

Detection of serum LPS and ALB concentration

Mouse serum LPS levels were detected using an ELISA kit, while serum ALB concentration was measured through the Bromocresol Green Colorimetric Method using the Cobas ® 8000 Modular Analyzer Series from Roche.

Statistical analysis

The results are presented as the mean with the standard deviation (± SEM) of the indicated number of replicates/experiments. We performed one-way analysis of variance to calculate the statistical differences among multiple groups followed by Uncorrected Fisher's LSD-ttest or performed paired comparisons through t test. An adjusted p-value of ≤ 0.05 was considered statistically significant.

Results

The COX2/PGE2 axis is co-related with Sj-induced liver fibrosis

Our previous studies have shown that the extent of hepatic fibrosis reached advanced levels at week (wk) 8 of *Sj* infection [27, 32]. To evaluate the correlation among COX2/PGE2 axis and hepatic fibrosis, the transcriptional level of *COX2, Ptges, Ptger1-4, Abcc4* and *Slco2a1* in mice liver were measured using RT-qPCR (Fig. 1a), and the translational level of COX2, mPGES-1 and EP1-4 in mice liver were detected by

western blotting (Fig. 1b) in 8-week *Sj*-infected and uninfected mice groups. Compared with the uninfected mice, the RNA expression level of *COX2, Ptges, Ptger1-4* and*Abcc4* significantly increased, while *Slco2a1*was significantly decreased (t-test: *wk 8vs* (-): COX2: $t_{(12)} = 5.690$, $P = 0.0001$; *Ptges*: $t_{(12)} = 9.702$, $P < 0.0001$; *Ptger1*: $t_{(12)} = 12.02$, $P < 0.0001$; *Ptger2*: $t_{(12)} = 9.783$, $p < 0.0001$; *Ptger3*: $t_{(12)} = 8.954$, $P < 0.0001$; *Ptger4*: $t_{(12)} = 9.550$, $P < 0.0001$; *Abcc4*: $t_{(12)} = 10.58$, $p < 0.0001$; *Slco2a1*: $t_{(12)} = 2.888$, $P = 0.0136$).Protein expression levels of COX2, mPGES-1and EP2, EP4 were also increased in wk 8 *Sj*-infected mice.

To assess whether the COX2/PGE2 axis is involved in the formation of liver fibrosis induced by *Sj* infection, we started to inject the COX2 inhibitor NS398 to *Sj*-infected mice at week 5 of infection. The whole treatment lasted for 3 weeks. NS398 treatment lowered the protein expression levels of COX2, mPGES-1, EP4 and α-SMA, Col I according to western blotting result (Fig. 2a, 2b) (t-test: DMSO/*Sj*(+) vs NS398/*Sj*(+): COX2: $t_{(8)} = 5.409$, $P = 0.0006$; mPGES-1: $t_{(8)} = 2.450$, $P = 0.0399$; EP4: $t_{(8)} = 2.660$, $P = 0.0288$; α-SMA: $t_{(8)} = 2.453$, $P = 0.0397$; COL1: $t_{(8)} = 2.569$, $P = 0.0332$), without significant change of EP2(t-test: DMSO/*Sj*(+) vs NS398/*Sj*(+): $t_{(8)} = 0.8025$,$P = 0.9534$). The expression of α-SMA changed from moderate to low level and Col I from high to moderate level according to Image J evaluated results. in the IHC assay (Fig. 2c-2f)(t-test: DMSO/*Sj*(+) vs NS398/*Sj*(+): α-SMA: $t_{(53)} = 3.437$, $P = 0.0012$; COL1: $t_{(34)} = 5.107$, $P < 0.0001$). In addition, the NS398-treated mice exhibited a significant reduction in the extent of collagen deposition after *Sj* infection (Fig. 2g, 2 h) (t-test: DMSO/*Sj*(+) vs NS398/*Sj*(+): $t_{(29)} = 3.681$, $P = 0.0010$). The average*Sj* eggs load in the per liver section showed the tendency to increase but without significant differences (Fig. 2i) (t-test: DMSO/*Sj*(+) vs NS398/*Sj*(+): $t(6) = 0.8619$, $P = 0.4218$). These indicated that the COX2/PGE2 axis is not only positively associated with CDAA-, TAA- and BDL-induced rat liver fibrosis [10, 11] and liver cirrhosis in rats, mice, and patients [9, 12], but also positively related with *Sj* infection-induced liver fibrosis.

TLR4 pathway activation stimulated the COX2/PGE2 axis, in Sj-infected mice andin LPS-exposed cultured HSCs

TLR4 signaling has been reported to induce HSCs activation and liver fibrosis through many mechanisms [22, 23]). The relationship of TLR4 and COX2/PGE2 axis in the *Sj*-infected liver is still unknown. To determine whether the TLR4 pathway regulates the COX2/PGE2 axis during *Sj* infection-induced liver fibrosis, we examined the levels of several key proteins in this axis using infected mice liver after TAK242 treatment. TAK242 treatment down-regulated the expression of mPGES-1, EP2, and EP4 in infected mice liver (Fig. 3a). Albumin (ALB) has been reported to trigger PGE2 degradation [9, 30]. Herein, the level of sera ALB was significantly lowered in the 8-week *Sj*-infected group compared to the non-infected one and TAK242 treatment did not reverse this reduction (Fig. 3b)(t-test, *Sj*(+) *vsSj*(-): $t_{(5)} = 5.932$, $P = 0.0019$). This observation rules out an implication of albumin in modulating PGE2 levels as a result of TLR4 pathway inhibition. Because *Sj* egg deposition increased the richness of microbiome in the gut of infected mice [33], we checked the level of LPS in serum, which might increase as a result from the larger quantities of Gram-negative bacteria in the gut. The concentration of serum LPS slightly increased gradually with *Sj*

infection (Fig. 3c) (Ordinary one-way ANOVA, $F_{(4, 5)} = 14.43$, $P = 0.0059$, followed by Uncorrected Fisher's LSD-ttest: wk 5 *vs* (-): $P = 0.7332$, wk 6 *vs* (-): $P = 0.2824$, *wk 8vs* (-): $P = 0.0196$, *wk 12vs* (-): $P = 0.0013$), likely to a too limited extent to produce a significant biological response.

To validate whether the TLR4 pathway regulates the COX2/PGE2 axis in the human HSCs line -LX-2, we examined the levels of several key proteins in this axis using cells exposed to LPS alone or after TAK242 treatment. COX2, mPGES-1, EP2 and EP4 were distinctly induced by LPS in a dose-dependent manner (Fig. 4a), and TAK242 pre-treatment gradually lowered these inductions, especially at a dose of 10uM (Fig. 4b).

In summary, our data are compatible with the model according to which TLR4 pathway activation stimulates the COX2/PGE2 axis, in *Sj*-infected mice andin LPS-exposed cultured HSCs.

Confirmation of the relationship between TLR4 signaling and HSCs activation & fibrogenesis

To verify the correlation between TLR4 signaling and HSCs activation and fibrogenesis, the LX-2 HSCs were employed and protein expression levels were monitored after exposure to LPS, or treatment with TAK242 or TLR4-specific siRNAs. LPS treatment from 1 ng/mL to 1ug/mL activated TLR4 signaling as monitored by the increased expression levels of TLR4 and p-p65, and the up-regulated protein expression of α-SMA and COL I (Fig. 5a). The protein levels of TLR4 and α-SMA in LPS-treated LX-2 (100 ng/ml) increased with the time of incubation (Fig. 5b). The increased TLR4, p-p65, α-SMA and COL I levels after LPS stimulation were reduced by TAK242 treatment, especially at a dose of 10uM (Fig. 5c). The up-regulation of α-SMA and COL I induced by LPS treatment were markedly decreased after TLR4-specific siRNA transfection (Fig. 5d). These data confirmed that TLR4 signaling is positively associated with HSCs activation and fibrogenesis.

The COX2/PGE2 axis was required for TLR4 signaling-induced HSCs activation and fibrogenesis

To assess the role of PGE2 in HSCs activation, we treated the LX-2 cell line with synthetic PGE2. HSCs activation was enhanced by synthetic PGE2 as monitored by the augmentation of α-SMA protein expression, while the expression of both EP2 and EP4 increased with the time of incubation (Fig. 6a). As reported in macrophages, intestinal epithelial cells, esophageal, and auditory cells [28, 29, 30, 31, 34], TLR4 signaling controls the activation of COX2-PGE2 pathway. Herein, we observed that in cultured HSCs, the activation of TLR4 signaling by LPS increased the protein expression levels of COX2, mPGES-1, EP2, EP4, α-SMA, and COL-I. These increased expression levels were reduced by NS398 treatment, especially at doses of 7.5uM and 10uM (Fig. 6b). Therefore, TLR4 signaling-dependent HSC activation and fibrogenesis is mediated at least partially through COX2/PGE2 axis.

Discussion

In this study, we investigated the relationship between COX2/PGE2 axis and TLR4 signaling in the induction of liver fibrosis in mice during *Sj* infection and in vitro culturing hepatic stellate cells. The COX2/PGE2 axis showed positive association with the extent of liver fibrosis induced by *Sj* infection.

TLR4 pathway activation stimulated the COX2/PGE2 axis, in *Sj*-infected mice liver tissue andin cultured HSCs.TLR4 signaling was certified to induce HSCs' activation and fibrogenesis in vitro, and COX2/PGE2 axis mediated this function. These indicated that liver fibrosis was induced by *Sj* infection through the activation of TLR4 signaling and then COX2/PGE2 axis.

Chronic liver inflammation leads to fibrosis and cirrhosis. Understanding the mechanisms of liver inflammation and fibrosis is critically important to develop treatments for liver diseases. Many reports have indicated that the COX2/PGE2 axis is positively associated with hepatic fibrogenesis[7, 8, 9, 10, 11, 12, 33]. Non-steroidal anti-inflammatory drugs inhibited the activity of COX and attenuated HSCs proliferation, contractility, and migration, thereby alleviating fibrogenesis[10].Efsen Eet aldemonstrated that NS398 inhibited MCP-1 expression via prostaglandin-cAMP pathway in TNF-α and IL-1β stimulated HSCs[35]. However, Hui AYet al[15]suggested that the COX2/PGE2 axis inhibits both basal and TGF-β1-mediated induction of collagen synthesis by another HSC cell line, LX-1 and primary HSCs. On a mouse model of CCl4 and BDL-induced liver fibrosis, COX2 expression in hepatocytes induces apoptosis of HSCs and attenuates liver fibrosis through PGE2 by down-regulating miR-23a-5p and miR-28a-5p[36]. Schippers M et al showed that PGE2 exerts anti-fibrotic activity by modulating cAMP effector Epac-1 production in HSCs, and a COX2 inhibitor-Niflumic acid effectively accentuated mice liver fibrosis induced by CCL4[37]. Herein, we showed that the components of COX2/PGE2axis were significantly up-regulated in *Sj*-infetected mice liver and in LPS-triggered HSCs. NS398 effectively attenuated both PGE2 synthesis and protein production of α-SMA and Col I. In the *Sj*-infected mice liver, increased expression of COX-2 and mPGES-1 induced synthesis, while high transcriptional level of MRP4 and low level of PGT would favor high levels of PGE2 in the liver microenvironment that may contribute to the overall liver fibrosis. The biological effects of PGE2 are mediated by EP1-EP4. EP2 and EP4 but not EP1 and EP3 showed high protein expression level in the *Sj*-infected mice liver, which suggested that PGE2's stimulating liver fibrosis through EP2 and EP4.

We had shown that TLR4 signaling in HSCs correlated with liver fibrosis post *Sj* infection [27]. As reported, TLR4 signaling controls the activation of COX2/PGE2 axis in several cell types[30, 31, 34, 38, 39]. The NF-κB pathway, activated by LPS-triggered TLR4 signaling, contributes to the early production of prostaglandins through the expression of COX2 and mPGES-1 in the macrophages [27].In the intestine, TLR4 signaling-mediated COX2-pathway activation through EP2 or EP4 was associated with proliferation and protection against apoptosis of intestinal epithelial cells [34].Our results showed that TLR4 pathway activation controls the expression of COX2, EP2&EP4, and synthesis of PGE2 in the HSCs. Importantly, lower expression levels of mPGES-1, EP2 & EP4 were detected in *Sj*-infected mice liver when TAK242 treatment. Serum albumin does not appear to affect PGE2 levels in a TLR4-dependent manner. Our results taken in the light of the previous work suggests that TLR4 pathway activation stimulated the COX2/PGE2 axis, in *Sj*-infected mice and in LPS-exposed cultured HSCs.

The current understanding of the role of COX2/PGE2 axis in liver fibrosis is limited by the varied effects observed depending on the model considered and the use of diverse PGE2 synthesis inhibitors. In this study, although the extent of liver fibrosis induced by *Sj* infection was strikingly reduced, egg load showed

the tendency of increasing. Moreover, *Sj*-infected mice with NS398 or TAK242 treatment manifested as fatigue and inappetence, which suggested that TLR4 signaling & COX2/PGE2 axis were required to protect against live *Sj* eggs. The medication time and dosage of these two inhibitors need to be carefully considered. Herein, we started to treat mice with NS398 in median dosageat wk 5 when the granulomatous inflammation existed for more than one week. Whether drug treatment in the late phase will obtained better effect or not needs further study. Anyway, the anti-fibrotic effect of this drug on *Sj*-infected mice in this studyis affirmative.

In this study, we confirmed that TLR4 signal pathway activation in HSCs was required for their activation and fibrogenesis, not only during *Sj* infection. The induction of endogenous PGE2 synthesis by LPS-triggered TLR4 pathway activation might play a role in HSCs activation since synthetic PGE2 induced α-SMA expression in LX-2 cells. High level of LPS-triggered TLR4 pathway activation and *Sj* infection positively controls the COX2/PGE2 axis and then subsequent HSC activation and fibrogenesis. NS398 was an effective inhibitor of this axis to alleviate liver fibrosis induced by TLR4 pathway activation and *Sj* infection. A worthy pursuit will be the study of the mechanisms downstream of PGE2-EP2&EP4 signaling.

Conclusions

Our study firstly outlined the reciprocal relationships between TLR4 signaling and the COX2/PGE2 axis and resulting HSC activation toward a fibrogenic phenotype. We also provide the evidence of TLR4 signaling activating the COX2/PGE2 axis that might contribute to mice liver fibrosis induced by *Sj* infection. The regulation of TLR4 signaling and COX2/PGE2 with a consequent decreasing of liver fibrosis may represent a potential therapeutic approach to hepatic granuloma caused by *Sj* infection.

Abbreviations

HSCs: hepatic stellate cells; Sj: Schistosoma japonicum; COX: cyclooxygenase; PGE2: prostanoid E2; α-SMA: alpha smooth muscle actin; COL I: collagen type I; TLR4: Toll like receptor 4; PGES: PGE2 synthases; mPGES: membrane-bound PGES; cPGES-1: cytosolic PGES-1; LPS: lipopolysaccharide; NF-κB: nuclear factor-kappa B; TAA**:** thioacetamide; BDL: bile duct ligation; ECM: extracellular matrix

Declarations

Ethics approval and consent to participate

Six to eight week old female C57BL/6 wild type mice were obtained from the SPF Biotechnology Co. Ltd (Beijing) and maintained in specific-pathogen-free (SPF) conditions. All mice were approved to be appropriate and humane by the Institutional Animal Care and Use Committee at South China Agricultural University (authorization no: 2019c013).

Consent for publication

Not applicable.

Availability of data and materials

The datasets supporting the conclusions of this article are included within the article.

Competing interests

The authors declare that they have no competing interests.

Funding

This work was funded by Provincial Natural Science Foundation of Guangdong (no. 2019A1515012171), the general project program of state key laboratory of respiratory disease (no. SKLRD-MS-201904) and the 111 Project (no. D18010).

Authors' contributions

LC, XFJ, MNW, XYX and ZCW performed the research. JJT, DF and ZL designed the research. LC, MNW, XYX and ZCW analyzed the data. LC, JJT and ZL wrote the paper, and DF and ZL revised the paper. All authors read and approved the final manuscript.

Acknowledgements

We acknowledge the expert technical help of Guiying Lin, Xiaomin Chang and Yaotang Wu.

References

1. Nakanishi M, Rosenberg DW. Multifaceted roles of PGE2 in inflammation and cancer. Semin Immunopathol.2013;35 2:123-37; doi: 10.1007/s00281-012-0342-8.
2. Kochel TJ, Goloubeva OG, Fulton AM. Upregulation of Cyclooxygenase-2/Prostaglandin E2 (COX-2/PGE2) Pathway Member Multiple Drug Resistance-Associated Protein 4 (MRP4) and Downregulation of Prostaglandin Transporter (PGT) and 15-Prostaglandin Dehydrogenase (15-PGDH) in Triple-Negative Breast Cancer. Breast cancer : basic and clinical research.2016;10:61-70; doi: 10.4137/bcbcr.s38529.
3. Jiang J, Dingledine R. Prostaglandin receptor EP2 in the crosshairs of anti-inflammation, anti-cancer, and neuroprotection. Trends Pharmacol Sci.2013;34 7:413-23; doi: 10.1016/j.tips.2013.05.003.
4. Kawahara K, Hohjoh H, Inazumi T, Tsuchiya S, Sugimoto Y. Prostaglandin E2-induced inflammation: Relevance of prostaglandin E receptors. Biochim Biophys Acta.2015;1851 4:414-21; doi: 10.1016/j.bbalip.2014.07.008. https://www.ncbi.nlm.nih.gov/pubmed/25038274.
5. Efsen E, Bonacchi A, Pastacaldi S, Valente AJ, Wenzel UO, Tosti-Guerra C, et al. Agonist-specific regulation of monocyte chemoattractant protein-1 expression by cyclooxygenase metabolites in

hepatic stellate cells. Hepatology.2001;33 3:713-21; doi: 10.1053/jhep.2001.22761. https://www.ncbi.nlm.nih.gov/pubmed/11230753.

6. Gallois C, Habib A, Tao J, Moulin S, Maclouf J, Mallat A, et al. Role of NF-kappaB in the antiproliferative effect of endothelin-1 and tumor necrosis factor-alpha in human hepatic stellate cells. Involvement of cyclooxygenase-2. The Journal of biological chemistry.1998;273 36:23183-90; doi: 10.1074/jbc.273.36.23183.
7. Cheng J, Imanishi H, Liu W, Iwasaki A, Ueki N, Nakamura H, et al. Inhibition of the expression of alpha-smooth muscle actin in human hepatic stellate cell line, LI90, by a selective cyclooxygenase 2 inhibitor, NS-398. Biochem Biophys Res Commun.2002;297 5:1128-34; doi: 10.1016/s0006-291x(02)02301-x.
8. Planaguma A, Claria J, Miquel R, Lopez-Parra M, Titos E, Masferrer JL, et al. The selective cyclooxygenase-2 inhibitor SC-236 reduces liver fibrosis by mechanisms involving non-parenchymal cell apoptosis and PPARgamma activation. FASEB journal : official publication of the Federation of American Societies for Experimental Biology.2005;19 9:1120-2; doi: 10.1096/fj.04-2753fje.
9. Gao JH, Wen SL, Tong H, Wang CH, Yang WJ, Tang SH, et al. Inhibition of cyclooxygenase-2 alleviates liver cirrhosis via improvement of the dysfunctional gut-liver axis in rats. Am J Physiol Gastrointest Liver Physiol.2016;310 11:G962-72; doi: 10.1152/ajpgi.00428.2015.
10. Paik YH, Kim JK, Lee JI, Kang SH, Kim DY, An SH, et al. Celecoxib induces hepatic stellate cell apoptosis through inhibition of Akt activation and suppresses hepatic fibrosis in rats. Gut.2009;58 11:1517-27; doi: 10.1136/gut.2008.157420.
11. Yamamoto H, Kondo M, Nakamori S, Nagano H, Wakasa K, Sugita Y, et al. JTE-522, a cyclooxygenase-2 inhibitor, is an effective chemopreventive agent against rat experimental liver fibrosis1. Gastroenterology.2003;125 2:556-71; doi: 10.1016/s0016-5085(03)00904-1.
12. O'Brien AJ, Fullerton JN, Massey KA, Auld G, Sewell G, James S, et al. Immunosuppression in acutely decompensated cirrhosis is mediated by prostaglandin E2. Nature medicine.2014;20 5:518-23; doi: 10.1038/nm.3516.
13. Penke LR, Huang SK, White ES, Peters-Golden M. Prostaglandin E2 inhibits alpha-smooth muscle actin transcription during myofibroblast differentiation via distinct mechanisms of modulation of serum response factor and myocardin-related transcription factor-A. The Journal of biological chemistry.2014;289 24:17151-62; doi: 10.1074/jbc.M114.558130.
14. Mohamed R, Jayakumar C, Ramesh G. Chronic administration of EP4-selective agonist exacerbates albuminuria and fibrosis of the kidney in streptozotocin-induced diabetic mice through IL-6. Laboratory investigation; a journal of technical methods and pathology.2013;93 8:933-45; doi: 10.1038/labinvest.2013.85.
15. Hui AY, Dannenberg AJ, Sung JJ, Subbaramaiah K, Du B, Olinga P, et al. Prostaglandin E2 inhibits transforming growth factor beta 1-mediated induction of collagen alpha 1(I) in hepatic stellate cells. J Hepatol.2004;41 2:251-8; doi: 10.1016/j.jhep.2004.04.033.

16. Brea R, Motino O, Frances D, Garcia-Monzon C, Vargas J, Fernandez-Velasco M, et al. PGE2 induces apoptosis of hepatic stellate cells and attenuates liver fibrosis in mice by downregulating miR-23a-5p and miR-28a-5p. Biochim Biophys Acta Mol Basis Dis.2018;1864 2:325-37; doi: 10.1016/j.bbadis.2017.11.001. https://www.ncbi.nlm.nih.gov/pubmed/29109031.
17. Puche JE, Saiman Y, Friedman SL. Hepatic stellate cells and liver fibrosis. Compr Physiol.2013;3 4:1473-92; doi: 10.1002/cphy.c120035. https://www.ncbi.nlm.nih.gov/pubmed/24265236.
18. Tsuchida T, Friedman SL. Mechanisms of hepatic stellate cell activation. Nat Rev Gastroenterol Hepatol.2017;14 7:397-411; doi: 10.1038/nrgastro.2017.38. https://www.ncbi.nlm.nih.gov/pubmed/28487545.
19. Tang J, Zhu X, Zhao J, Fung M, Li Y, Gao Z, et al. Tissue Transglutaminase-Regulated Transformed Growth Factor-β1 in the Parasite Links Schistosoma japonicum Infection with Liver Fibrosis. Mediators of inflammation.2015;2015:659378; doi: 10.1155/2015/659378.
20. Seki E, Schwabe RF. Hepatic inflammation and fibrosis: functional links and key pathways. Hepatology.2015;61 3:1066-79; doi: 10.1002/hep.27332. https://www.ncbi.nlm.nih.gov/pubmed/25066777.
21. Aoyama T, Paik YH, Seki E. Toll-like receptor signaling and liver fibrosis. Gastroenterology research and practice.2010;2010; doi: 10.1155/2010/192543.
22. Seki E, De Minicis S, Osterreicher CH, Kluwe J, Osawa Y, Brenner DA, et al. TLR4 enhances TGF-beta signaling and hepatic fibrosis. Nature medicine.2007;13 11:1324-32; doi: 10.1038/nm1663.
23. Liu C, Chen X, Yang L, Kisseleva T, Brenner DA, Seki E. Transcriptional repression of the transforming growth factor beta (TGF-beta) Pseudoreceptor BMP and activin membrane-bound inhibitor (BAMBI) by Nuclear Factor kappaB (NF-kappaB) p50 enhances TGF-beta signaling in hepatic stellate cells. The Journal of biological chemistry.2014;289 10:7082-91; doi: 10.1074/jbc.M113.543769.
24. Roderburg C, Urban GW, Bettermann K, Vucur M, Zimmermann H, Schmidt S, et al. Micro-RNA profiling reveals a role for miR-29 in human and murine liver fibrosis. Hepatology.2011;53 1:209-18; doi: 10.1002/hep.23922. https://www.ncbi.nlm.nih.gov/pubmed/20890893.
25. Seki E, De Minicis S, Gwak GY, Kluwe J, Inokuchi S, Bursill CA, et al. CCR1 and CCR5 promote hepatic fibrosis in mice. The Journal of clinical investigation.2009;119 7:1858-70; doi: 10.1172/jci37444.
26. Zhang Z, Lin C, Peng L, Ouyang Y, Cao Y, Wang J, et al. High mobility group box 1 activates Toll like receptor 4 signaling in hepatic stellate cells. Life sciences.2012;91 5-6:207-12; doi: 10.1016/j.lfs.2012.07.009.
27. Wen Z, Ji X, Tang J, Lin G, Xiao L, Liang C, et al. Positive Feedback Regulation between Transglutaminase 2 and Toll-Like Receptor 4 Signaling in Hepatic Stellate Cells Correlates with Liver Fibrosis Post Schistosoma japonicum Infection. Frontiers in immunology.2017;8:1808; doi: 10.3389/fimmu.2017.01808.
28. Zhang Y, Igwe OJ. Lipopolysaccharide (LPS)-mediated priming of toll-like receptor 4 enhances oxidant-induced prostaglandin E2 biosynthesis in primary murine macrophages. Int

Immunopharmacol.2018;54:226-37; doi: 10.1016/j.intimp.2017.11.017. https://www.ncbi.nlm.nih.gov/pubmed/29161659.

29. Samuchiwal SK, Balestrieri B, Raff H, Boyce JA. Endogenous prostaglandin E2 amplifies IL-33 production by macrophages through an E prostanoid (EP)2/EP4-cAMP-EPAC-dependent pathway. The Journal of biological chemistry.2017;292 20:8195-206; doi: 10.1074/jbc.M116.769422. https://www.ncbi.nlm.nih.gov/pubmed/28341741.
30. Verbeek RE, Siersema PD, Ten Kate FJ, Fluiter K, Souza RF, Vleggaar FP, et al. Toll-like receptor 4 activation in Barrett's esophagus results in a strong increase in COX-2 expression. J Gastroenterol.2014;49 7:1121-34; doi: 10.1007/s00535-013-0862-6. https://www.ncbi.nlm.nih.gov/pubmed/23955118.
31. Tanigawa T, Odkhuu E, Morikawa A, Hayashi K, Sato T, Shibata R, et al. Immunological role of prostaglandin E2 production in mouse auditory cells in response to LPS. Innate Immun.2014;20 6:639-46; doi: 10.1177/1753425913503578. https://www.ncbi.nlm.nih.gov/pubmed/24055878.
32. Tang J, Huang H, Ji X, Zhu X, Li Y, She M, et al. Involvement of IL-13 and tissue transglutaminase in liver granuloma and fibrosis after schistosoma japonicum infection. Mediators of inflammation.2014;2014:753483; doi: 10.1155/2014/753483.
33. Zhao Y, Yang S, Li B, Li W, Wang J, Chen Z, et al. Alterations of the Mice Gut Microbiome via Schistosoma japonicum Ova-Induced Granuloma. Front Microbiol.2019;10:352; doi: 10.3389/fmicb.2019.00352.
34. Fukata M, Chen A, Klepper A, Krishnareddy S, Vamadevan AS, Thomas LS, et al. Cox-2 is regulated by Toll-like receptor-4 (TLR4) signaling: Role in proliferation and apoptosis in the intestine. Gastroenterology.2006;131 3:862-77; doi: 10.1053/j.gastro.2006.06.017.
35. Chen CC. Signal transduction pathways of inflammatory gene expressions and therapeutic implications. Current pharmaceutical design.2006;12 27:3497-508; doi: 10.2174/138161206778343028.
36. Brea R, Motiño O, Francés D, García-Monzón C, Vargas J, Fernández-Velasco M, et al. PGE(2) induces apoptosis of hepatic stellate cells and attenuates liver fibrosis in mice by downregulating miR-23a-5p and miR-28a-5p. Biochimica et biophysica acta Molecular basis of disease.2018;1864 2:325-37; doi: 10.1016/j.bbadis.2017.11.001.
37. Schippers M, Beljaars L, Post E, Lotersztajn S, Reker-Smit C, Han B, et al. Upregulation of Epac-1 in Hepatic Stellate Cells by Prostaglandin E(2) in Liver Fibrosis Is Associated with Reduced Fibrogenesis. The Journal of pharmacology and experimental therapeutics.2017;363 2:126-35; doi: 10.1124/jpet.117.241646.
38. Zhang Y, Igwe OJ. Lipopolysaccharide (LPS)-mediated priming of toll-like receptor 4 enhances oxidant-induced prostaglandin E(2) biosynthesis in primary murine macrophages. Int Immunopharmacol.2018;54:226-37; doi: 10.1016/j.intimp.2017.11.017.
39. Samuchiwal SK, Balestrieri B, Raff H, Boyce JA. Endogenous prostaglandin E(2) amplifies IL-33 production by macrophages through an E prostanoid (EP)(2)/EP(4)-cAMP-EPAC-dependent pathway.

The Journal of biological chemistry.2017;292 20:8195-206; doi: 10.1074/jbc.M116.769422.

Figures

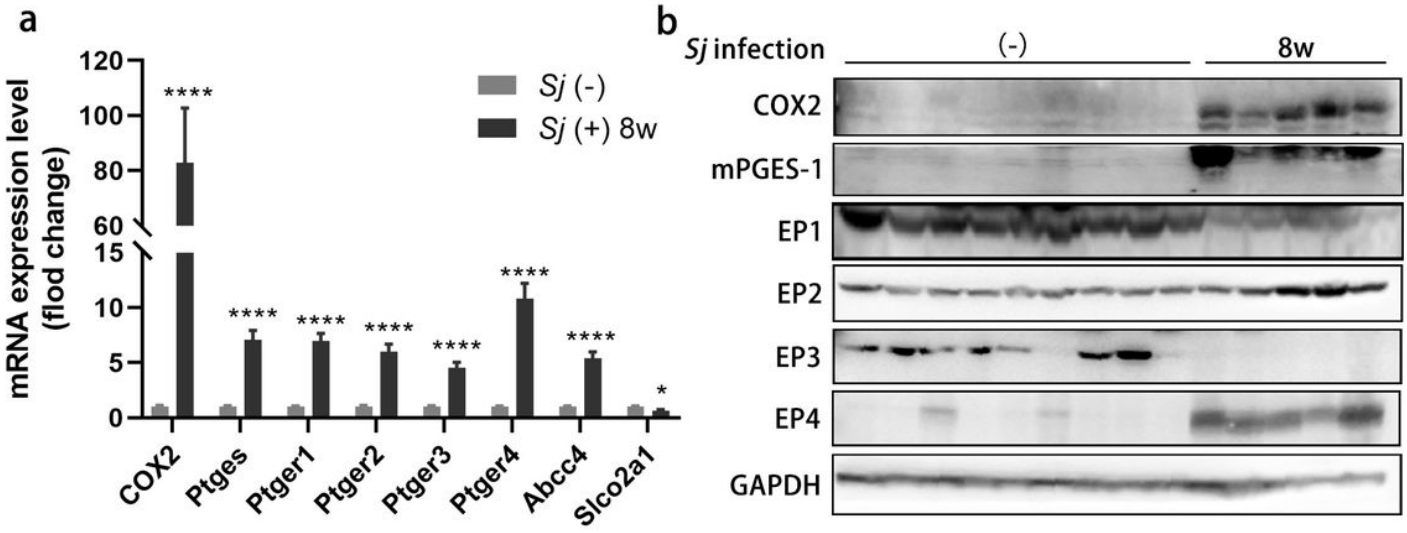

Figure 1

The components of COX2/PGE2 axis are overexpressed in the liver of mice with 8-week Sj infection. C57BL/6 mice were infected with 20 ± 3 cercariae of Sj for 0 or 8 weeks. Mice liver samples were kept in Trizol or in RIPA for RNA or total protein extraction respectively. a The relative RNA expression level of COX2, Ptges, Ptger1-4, Abcc4 and Slco2a1 in indicated mice liver were measured using RT-qPCR. Gapdh acts as an internal control (t-test, *p< 0.05, ****P < 0.0001). b The protein expression level of COX2, mPGES-1 and EP1-4 in mice liver homogenates were detected by Western blotting. GAPDH is used as a loading control. Data are presented as mean± SEM from 5 mice in Sj infection group and 9 mice in non-infection group.

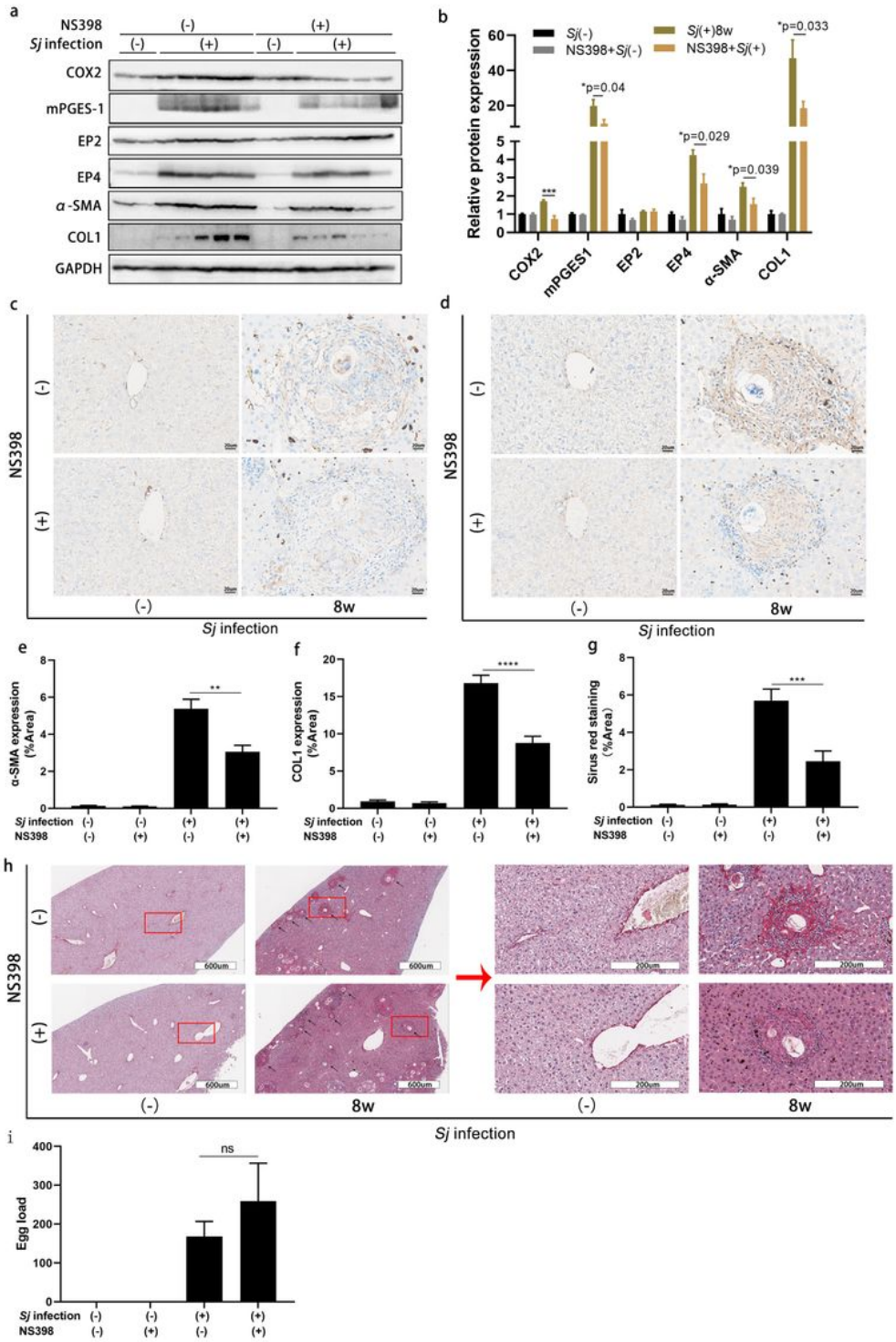

Figure 2

Suppression of COX2 activity with NS398 consistently diminished the expression level of the components of COX2/PGE2 axis and the extent of hepatic fibrosis. The activity of COX2 in mice was inhibited by NS398 through intraperitoneal injection 3 times per week from Week 5 to Week 7 after Sj infection. Mice were sacrificed at week 8. Non-infected mice with or without NS398 treatment served as controls. a and b The protein expression level of COX2, mPGES-1, EP2, EP4 and α-SMA, Col I in mice liver homogenates

detected by Western blotting was displayed in (a), and semi-quantitative result was shown in (b) (t-test, **p< 0.01, ***P < 0.001). GAPHD was used as loading control. c-f The protein expression levels and location of α-SMA (c) and Col I (d)in mice liver tissue were determined by IHC assay (200×), and the semi-quantitative result of these proteins was shown using Image J analysis in (e) (t-test, **p< 0.01) and (f) (t-test, ****P < 0.0001). The percentage of morphometric collagen areas of single Sj egg granuloma was shown in (g) (t-test, ***P < 0.001). Representative Sirius red staining (200×) of Sj single egg granuloma is shown in (h). i The average Sj egg number on each liver section was shown (t-test, ns, no significance). Data were presented as mean ±SEM from 5-9 mice per group.

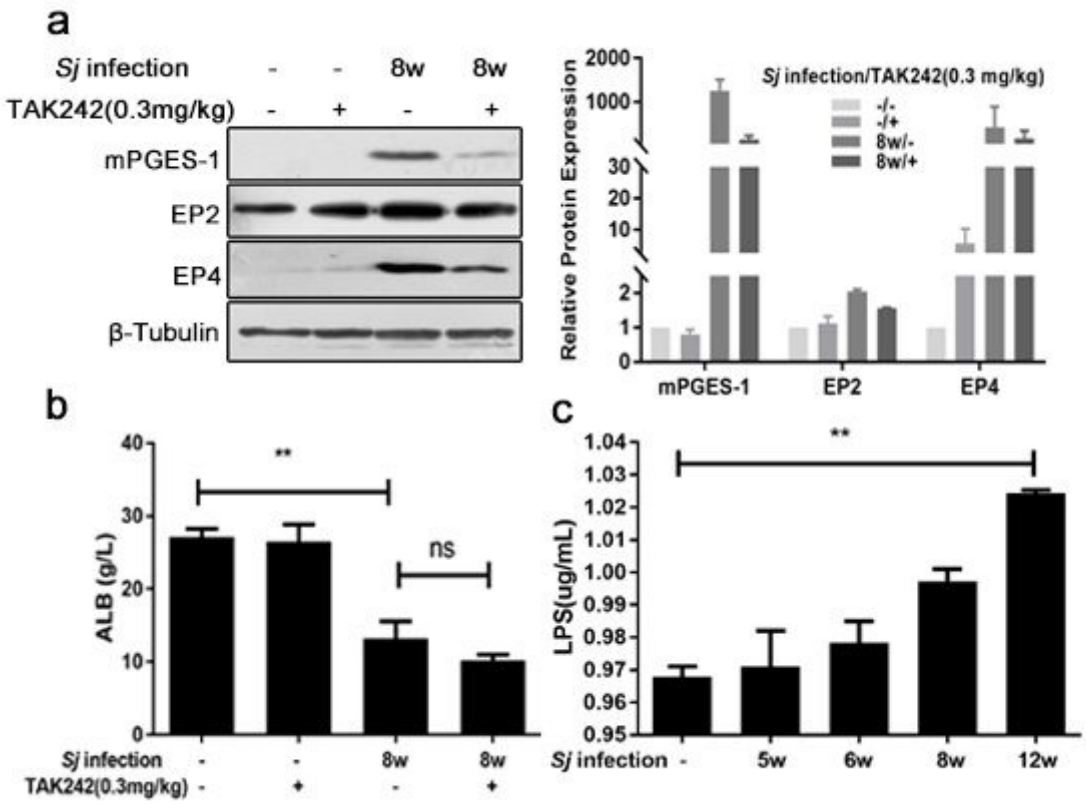

Figure 3

TLR4 pathway activation stimulated the COX2/PGE2 axis in Sj-infected mice. TLR4 signaling in C57BL/6 mice was inhibited by intraperitoneal injection of TAK242 once a day from week 4 to 8 post Sj infection. a and b The protein expression level of mPGES-1, EP2 and EP4 in mice liver homogenates tested by Western blotting was shown in (a left), and semi-quantitative result was displayed in (a right). b Concentration of sera ALB of TAK242 treated or untreated mice with or without Sj infection was detected by Bromocresol Green Colorimetric Method (t-test, **P < 0.01, ns, no significance). c Concentration of LPS in sera of mice with indicated time courses was detected by ELISA (Ordinary one-way ANOVA, **P < 0.01). Data are presented as mean ± SEM from 7–10 mice per group. All experiments were performed twice.

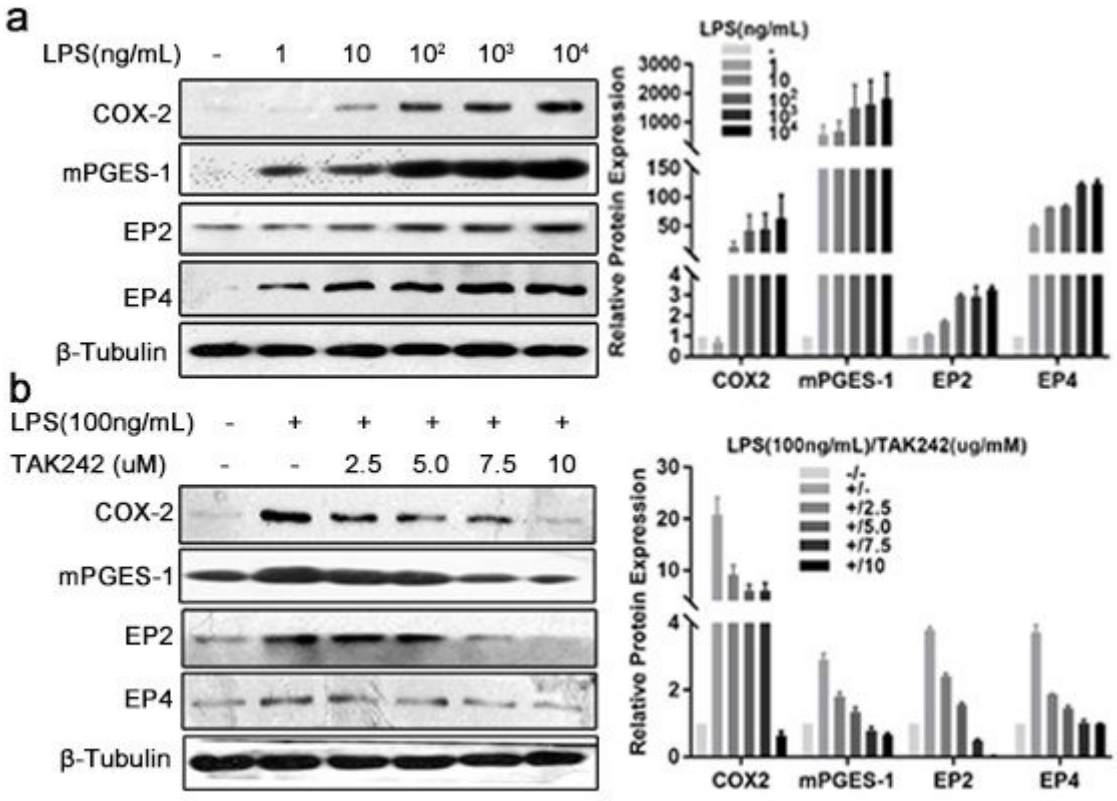

Figure 4

TLR4 pathway activation stimulated the COX2/PGE2 axis in cultured HSCs. a The hepatic stellate cell lineLX-2 cells were triggered with LPS for indicated concentrations for 24h, the protein expression level of COX2, mPGES-1, EP2 and EP4 detected by Western blotting was displayed on the left panel, and semi-quantitative result was shown on the right panel.b. LX-2 cells were pretreated with TAK242 for indicated concentrations for 30min prior to stimulation with LPS (100ng/ml) for 24h. Non-treatment or LPS (100ng/ml) treatment alone were settled as controls. Indicated protein expression levels were evaluated by western blotting as shown in left panel, and the semi-quantitative result was shown in right panel. β-Tubulin was used as a loading control. Each experiment was conducted for two or three times.

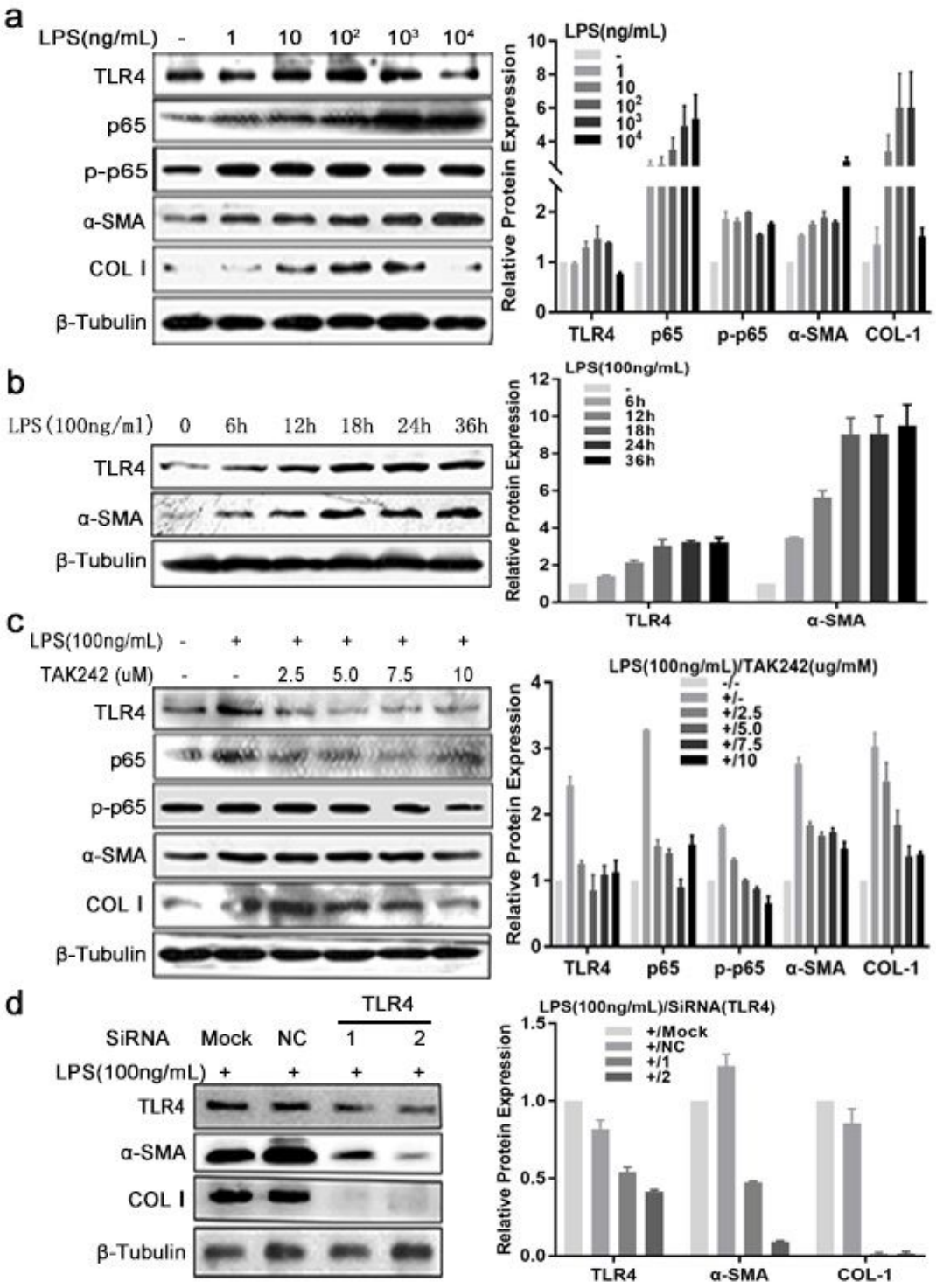

Figure 5

TLR4 signaling was verified to induce hepatic stellate cells' activation and fibrogenesis in vitro. a LX-2 was triggered with different doses of LPS for 24h orwas triggered with LPS (100ng/ml) for indicated time courses. b/c LX-2 cells were pretreated with TAK242 for indicated concentrations for 30min prior to stimulation with LPS (100ng/ml) for 24h. Non-treatment or LPS treatment alone were settled as controls. d LX-2 cells were transfected with either control siRNA (NC) or 2 different TLR4 siRNA and cultured for

24h, and then stimulated with LPS (100ng/ml) for 24h. Indicated protein expression levels were determined using western blotting as shown in left panels, and the semi-quantitative results were shown in right panels. Each experiment was conducted at least twice. β-Tubulin was used as a loading control.

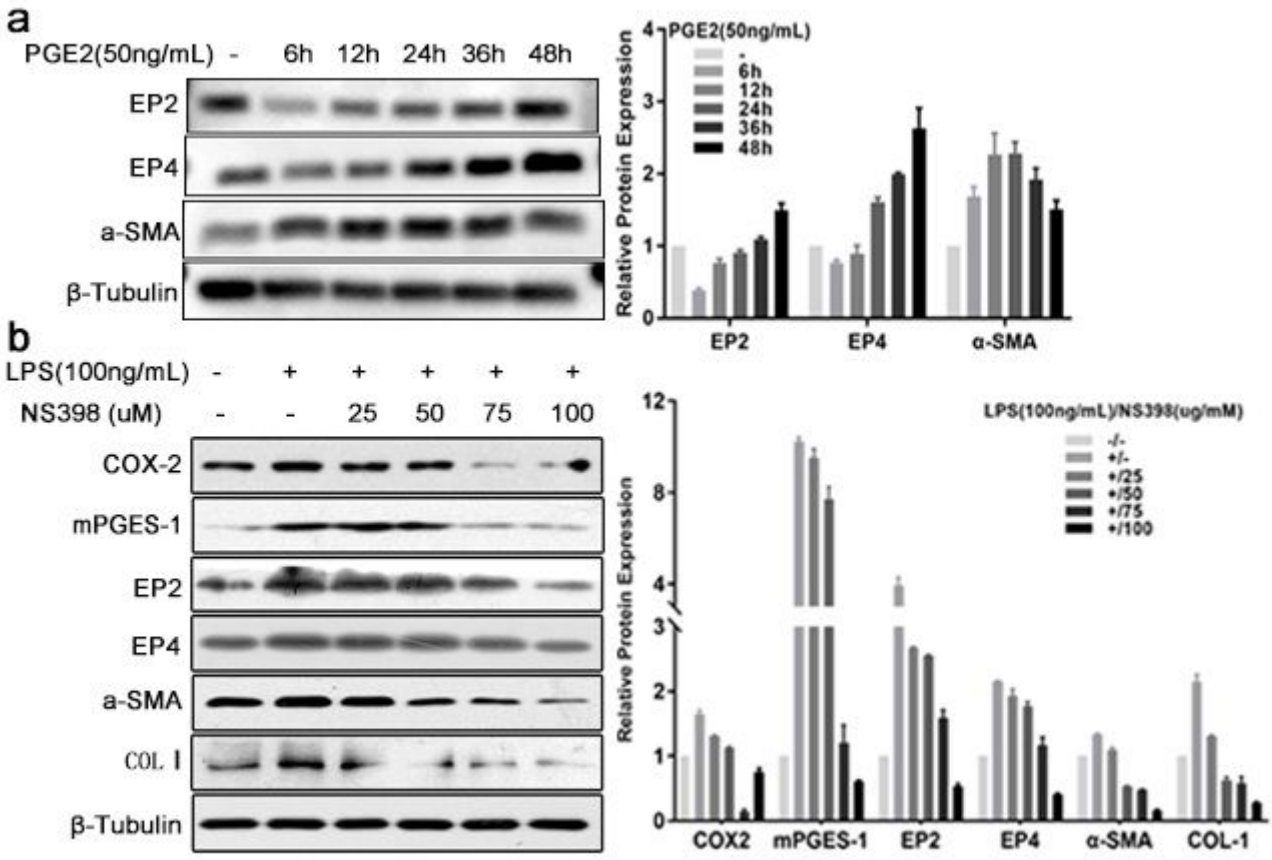

Figure 6

COX2/PGE2 axis induced LPS-operated HSCs activation & fibrogenesis in vitro. a LX-2 cells were triggered with synthetic PGE2 (50ng/ml) for indicated times. b LX-2 cells were pretreated with NS398 for indicated concentrations for 15min prior to stimulation with LPS (100ng/ml) for 24h. Non-treatment or LPS (100ng/ml) treatment alone were settled as controls. Indicated protein expression levels were evaluated by western blotting as shown on the left panels, and the semi-quantitative results were shown on the right panels. β-Tubulin was used as a loading control. Each experiment was conducted for two or three times.

Supplementary Files

This is a list of supplementary files associated with this preprint. Click to download.

- GraphicalAbstract.png